Required Accuracy of MR-US Registration for Prostate Biopsies

Wendy J.M. van de Ven, Geert J.S. Litjens, Jelle O. Barentsz, Thomas Hambrock, and Henkjan J. Huisman

Department of Radiology,
Radboud University Nijmegen Medical Centre,
Nijmegen, The Netherlands
W.vandeVen@rad.umcn.nl

Abstract. MR to TRUS guided biopsies can be a cost-effective solution for prostate biopsies. Prostate cancer can be detected on MRI and a biopsy can be directed towards a suspicious region. With the help of an accurate MR-US registration method the tumor can also be targeted under transrectal US guidance. For heterogeneous tumors, the needle should be guided towards the most aggressive part of the tumor. Not the tumor size, but the size of this smaller tumor hotspot determines the required accuracy of the registration. We investigate the percentage of tumors that are heterogeneous and the corresponding hotspot volume. Results show a hotspot in 63% of the tumors, with a median volume of 0.3 cm^3. By assuming a spherical shape, the required accuracy can be determined. For a 90% tumor hit-rate, the registration error should be less than 2.87 mm.

Keywords: MR-US registration, accuracy, hotspot, prostate biopsy.

1 Introduction

Prostate cancer is the second most common diagnosed malignancy in men in the western world, and one of the leading causes of death from cancer [7]. The current routine clinical standard method for making a definite diagnosis of prostate cancer is transrectal ultrasound (TRUS) guided biopsy. Prostate cancer is not visible on gray-scale ultrasound, thus TRUS is merely used to guide systematic biopsies. This systematic approach misses nearly a quarter of detectable cancers on the first biopsy [15]. Furthermore it underestimates the true Gleason score compared to radical prostatectomy specimens [12]. So the number of detected aggressive tumors is rather low with TRUS guided biopsy.

Magnetic resonance (MR) guided MR biopsy is a very promising technique for prostate biopsies. Firstly, multiparametric MR imaging (MRI) has proven to be an effective technique to detect prostate cancer. A combination of anatomical T2 weighted MRI, dynamic contrast enhanced MRI, and diffusion weighted MRI (DWI) improves the accuracy of prostate cancer localization over T2 weighted imaging alone [11,18]. Secondly, it has been shown that MR guided biopsy significantly increases the tumor detection rate as compared to TRUS systematic

A. Madabhushi et al. (Eds.): Prostate Cancer Imaging 2011, LNCS 6963, pp. 92–99, 2011.

biopsy [3]. Additionally, recent research has investigated the correlation between DWI and tumor aggressiveness. The apparent diffusion coefficient (ADC) determined at MRI has proven to be inversely correlated to the Gleason grade in peripheral zone prostate cancer [1,4,6]. It has moreover been shown that DWI guided biopsy determines Gleason grading in exact concordance with prostatectomy in 88% of the cases, which is substantially higher than TRUS systematic biopsy (55%) [2]. However, disadvantages of MR guided MR biopsy are that MRI is not widely available. It is also a relatively expensive method for taking prostate biopsies; the patient needs a detection MRI scan but then also a second MRI scan for guiding the biopsy.

An alternative is MR guided TRUS biopsy. MRI will still be used for the detection and localization of prostate cancer. These images can then enhance TRUS imaging and improve needle guidance, thereby taking advantages of both modalities. Accurate MR-TRUS registration is difficult and topic of current research. Recent works have investigated several MR to US registration methods, including rigid as well as nonrigid methods. Reported root mean square (RMS) target registration errors (TREs) lie within the range of $1.5-3.3$ mm [5,9,13,16]. However, these studies only look at the root mean square distance between TRUS-based and MRI-based segmentations of the prostate. Clinical studies using rigid fusion reported a significantly increased detection rate upon targeted prostate biopsy with MR-US fusion [8,14]. But there is to date no clinical study investigating the Gleason grading with MR guided TRUS biopsies. Accurate Gleason grading depends on accurate targeting of biopsies in the most aggressive tumor part.

In this paper, we investigate the required accuracy of the registration. To our knowledge, the current required accuracy is based on the widely used cutoff value of 0.5 cm^3 for clinically significant tumor volumes [5,9]. Some of the clinically significant tumors are heterogeneous, with only part of the volume containing highest Gleason grade tumor. For a correct grading, the biopsy needs to be targeted to the high-grade tumor volume part, thus requiring a higher registration accuracy. The required accuracy depends on the size of the most aggressive tumor part, the so-called tumor 'hotspot'. As aggressiveness showed an inverse relationship with ADC values, we define the darkest tumor region on the ADC map as tumor hotspot. We determine the hotspot sizes, as these are not yet known. We first investigate how many tumors are heterogeneous. Secondly, in case of a heterogeneous tumor, we determine the volume of the most aggressive part of the tumor. Using this hotspot volume, we estimate the required maximal registration error for taking a representative biopsy under MR to TRUS guidance.

2 Methods

2.1 Patient Data

For this study we used a dataset containing 51 consecutive patients with 62 different peripheral zone tumors, who where scheduled for radical prostatectomy between August 2006 and January 2009 [4]. Multiparametric MR imaging was

performed at a 3.0-T MR system (Trio Tim; Siemens, Erlangen, Germany). Water diffusion was measured in three directions using b values of 0, 50, 500, and 800 s mm^{-2}. The ADC maps were automatically calculated by the imager software using all four b values.

After radical prostatectomy, prostate specimens were uniformly processed and entirely submitted for histologic investigation. Gleason grade and pathologic stage were determined for each individual tumor (see [4] for a summary of clinical characteristics). The entire tumor volume was outlined on each step-section. MR images were carefully aligned to these histopathologic step-sections. Regions of interest were then retrospectively annotated on the ADC map (Figs. 1a-e).

2.2 Automatic Hotspot Detection and Segmentation

The annotated ADC maps are used for an automatic detection of tumor hotspots. First, it is evaluated if the tumor is heterogeneous and thus contains a tumor hotspot. Second, the hotspot is automatically segmented and its volume can be determined.

The tumor hotspot is defined as the most aggressive part of the tumor, corresponding to the darkest region on the ADC map. We distinguished this region by an upper threshold of 1.07×10^{-3} mm^2 s^{-1}, which is based on Hambrock et al. [4]. This way, most of the high-grade tumors and half of the intermediate-grade tumors can be differentiated. To reduce image noise, a 3D Gaussian smoothing filter ($\sigma = 0.50$) is applied to the ADC map before analysis.

A tumor hotspot can be detected if the tumor contains a substantial amount of voxels both below and above the threshold of 1.07×10^{-3} mm^2 s^{-1}. We recorded a hotspot if its volume was between 5% and 95% of the total tumor volume. In this case the tumor is heterogeneous. Two types of homogeneous tumors can be distinguished: a tumor with almost all ADC values above the threshold (hotspot $< 5\%$) and a tumor with most values below this threshold (hotspot $> 95\%$).

When a hotspot is detected, a segmentation is needed before estimating its volume. The segmentation of the hotspot is done by means of a region growing, taking the minimum ADC value within the annotated region as seed point. In order to prevent leakage outside the tumor, the region growing is limited by the boundaries of the annotation (Fig. 1f).

2.3 Registration Accuracy

The required accuracy of MR-US registration methods depends on the smaller hotspot volume, not on the total tumor volume. Assuming that the tumor hotspot has a spherical shape, its volume can be used to determine its radius. Assuming negligible needle deflection, the tumor can be targeted when the TRE of the method is less than the radius.

By applying a procedure similar as described in Hu et al. [5], the clinical need for a TRE can be derived for a specified tumor hit-rate. Therefore, we furthermore assume that the targeting error is normally distributed and follows

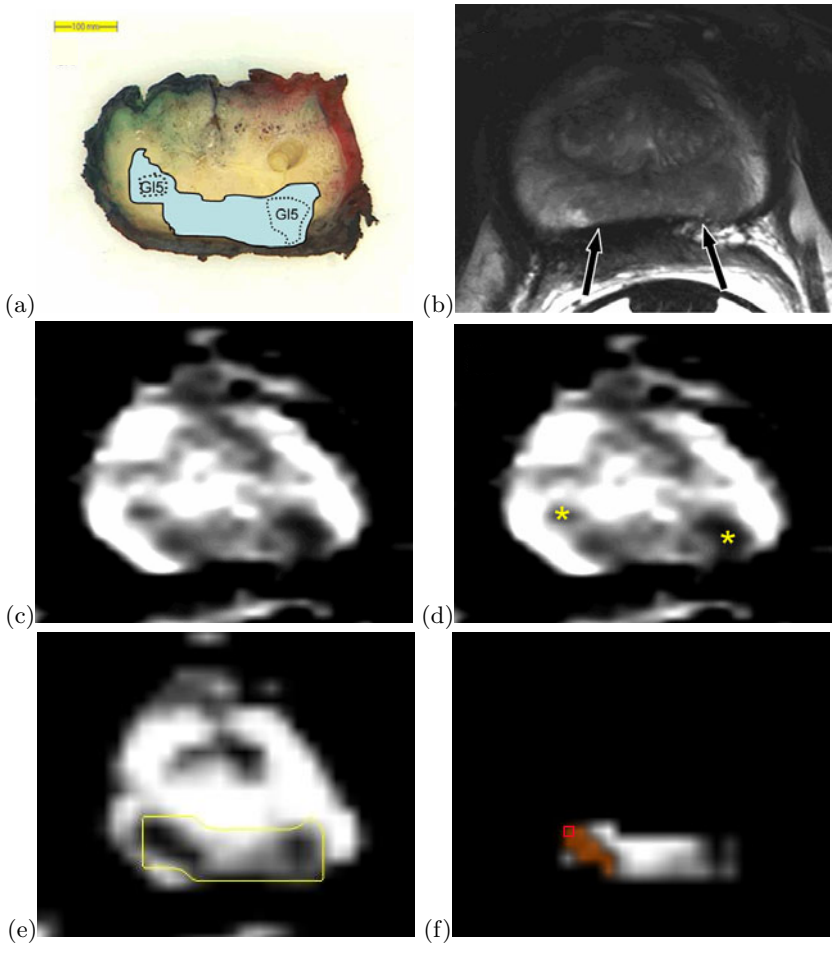

Fig. 1. Patient with a peripheral zone tumor revealing Gleason 3 + 4 + 5 on final pathology. (a) Prostatectomy step-section with the tumor delineated in light blue. Regions with focal Gleason grade 5 on pathology are delineated with a dotted line. (b) Anatomical T2 weighted MR image. A large tumor region corresponding to the step-section is shown in the peripheral zone as indicated by the arrows. (c) On the ADC map, water restriction is clearly visible for the same lesion. (d) The Gleason 5 components are visible as dark regions (yellow asterisks). (e) Regions of interest annotated on the smoothed ADC map in correspondence with prostatectomy step-section (yellow delineation). (f) The segmentation of the hotspot finding based on ADC values (orange region). The red square indicates the seed point for the region growing.

a Maxwell-Boltzmann probability density function. The RMS TRE is then equal to $\sqrt{3}\sigma$. By determining the σ corresponding to the radius and the specified hit-rate, the threshold on the RMS TRE can be derived.

3 Results

Of the 62 peripheral zone tumors, 62.9% (39/62) were heterogeneous, 27.4% (17/62) had no hotspot at all, and 9.7% (6/62) were entirely dark on the ADC map. The numbers and volumes for each type are shown in Fig. 2. The heterogeneous tumors are somewhat larger than both homogeneous types, but not significantly different.

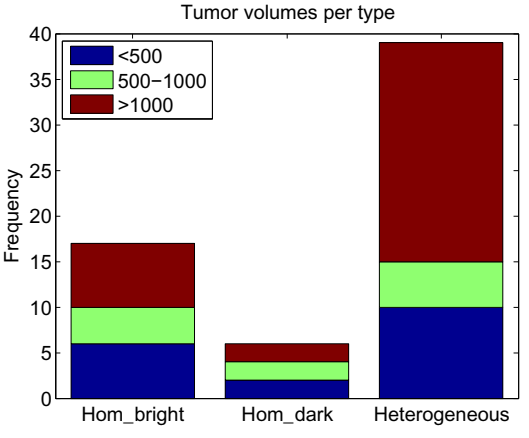

Fig. 2. Number of tumors for each type: homogeneous bright, homogeneous dark, and heterogeneous. Three volume ranges are indicated: $0-500$ mm^3, $500-1000$ mm^3, and > 1000 mm^3.

The heterogeneous tumors are important for determining the volume of the tumor hotspot. For these tumors, a boxplot for both the total tumor volume and the hotspot volume is shown in Fig. 3a. The distribution of the hotspot volumes is shown in a histogram in Fig. 3b. It can be seen that most of the hotspot volumes are below 500 mm^3, with a median of 297 mm^3.

For the estimation of the registration accuracy, we take the median tumor hotspot volume. The radius of a sphere with a volume of 297 mm^3 is 4.14 mm. For a tumor hit-rate of 90%, the threshold on the target registration error is 2.87 mm. Fig. 4a shows a graph of the TRE threshold as a function of the tumor hit-rate for the median hotspot volume. We also estimated the TRE threshold as a function of the hotspot volume for a fixed tumor hit-rate of 90% (Fig. 4b).

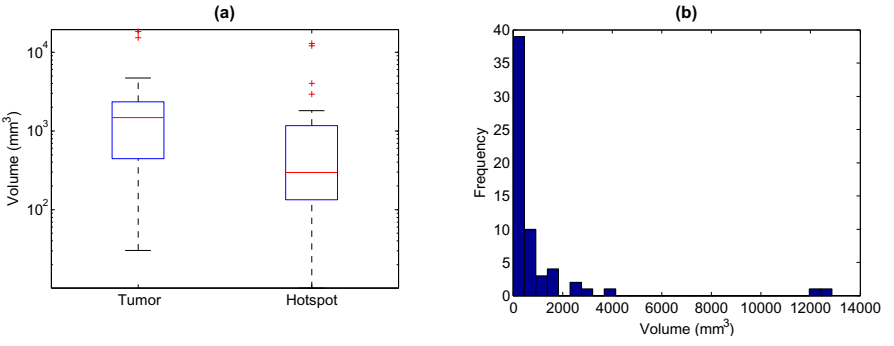

Fig. 3. (a) Boxplot showing the hotspot volumes in comparison with the total tumor volumes for heterogeneous tumors. (b) Distribution of the tumor hotspot volumes.

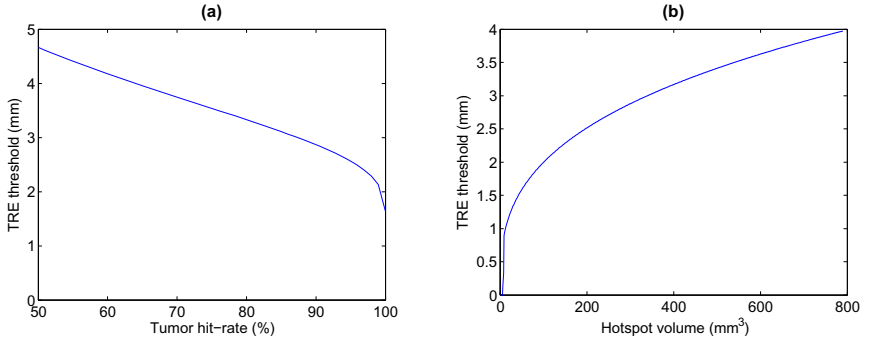

Fig. 4. (a) The TRE threshold as a function of the tumor hit-rate for the median tumor hotspot volume. (b) The TRE threshold as function of the hotspot volume for a 90% tumor hit-rate.

4 Discussion

We have shown that 62.9% of the peripheral zone tumors contain a hotspot. The median hotspot volume is 297 mm^3. To correctly assess the aggressiveness of the tumor, an accuracy of 2.87 mm is required (for the median volume and a 90% hit-rate).

However, there are some limitations to this study. First, the dataset is biased in that it only contains patients who are already scheduled for a prostatectomy. The tumors investigated are thus relatively large and aggressive. If data from a screening group would be taken, the mean tumor size will most likely decrease. The TRE threshold might then even be lower than 2.87 mm. Second, transition zone tumors were excluded. Transition zone tumors are known to have different ADC values than peripheral zone tumors [10,17]. Therefore, another threshold might be needed for the hotspot detection in this zone. Third, we took the median hotspot volume for estimating the required registration accuracy. By taking this

value, we did not take into account the lower half of the tumor hotspots volumes. For smaller volumes, the TRE decreases as shown in Fig. 4b. So for increasing the hotspot detection rate for the smaller hotspots, the registration error should also be smaller. Furthermore, we only detected one hotspot per tumor. The example illustrated in Fig. 1 contains two hotspots of which only one was detected. This will increase the number of hotspots, but not the required accuracy.

Future work will focus on an accurate MR-US registration method (Toshiba Aplio XG ultrasound machine). The Gleason grading with MR guided TRUS biopsies and its correspondence with radical prostatectomy specimens can be investigated. It might also be interesting to explore the sizes of tumor hotspots on prostatectomy specimens and its correspondence with DWI.

References

1. de Souza, N.M., Riches, S.F., Vanas, N.J., Morgan, V.A., Ashley, S.A., Fisher, C., Payne, G.S., Parker, C.: Diffusion-weighted magnetic resonance imaging: a potential non-invasive marker of tumour aggressiveness in localized prostate cancer. Clin. Radiol. 63(7), 774–782 (2008)
2. Hambrock, H., Hoeks, C., Scheenen, T., Fütterer, J.J., Bouwense, S., van Oort, I., Schröder, F., Huisman, H.J., Barentsz, J.O.: Prospective assessment of prostate cancer aggressiveness using 3 Tesla diffusion weighted MR imaging guided biopsies versus a systematic 10-core transrectal ultrasound prostate biopsy cohort. Eur. Urol (submitted 2011)
3. Hambrock, T., Somford, D.M., Hoeks, C., Bouwense, S.A.W., Huisman, H., Yakar, D., van Oort, I.M., Witjes, J.A., Fütterer, J.J., Barentsz, J.O.: Magnetic resonance imaging guided prostate biopsy in men with repeat negative biopsies and increased prostate specific antigen. J. Urol. 183(2), 520–527 (2010)
4. Hambrock, T., Somford, D.M., Huisman, H.J., van Oort, I.M., Witjes, J.A., van de Kaa, C.A.H., Scheenen, T., Barentsz, J.O.: Relationship between apparent diffusion coefficients at 3.0-T MR imaging and Gleason grade in peripheral zone prostate cancer. Radiology 259(2), 453–461 (2011)
5. Hu, Y., Ahmed, H.U., Taylor, Z., Allen, C., Emberton, M., Hawkes, D., Barratt, D.: MR to ultrasound registration for image-guided prostate interventions. Med. Image Ana. (in Press 2011) (accepted Manuscript)
6. Itou, Y., Nakanishi, K., Narumi, Y., Nishizawa, Y., Tsukuma, H.: Clinical utility of apparent diffusion coefficient (ADC) values in patients with prostate cancer: can ADC values contribute to assess the aggressiveness of prostate cancer? J. Magn. Reson. Imaging 33(1), 167–172 (2011)
7. Jemal, A., Bray, F., Center, M.M., Ferlay, J., Ward, E., Forman, D.: Global cancer statistics. CA Cancer J. Clin. 61(2), 69–90 (2011)
8. Kadoury, S., Yan, P., Xu, S., Glossop, N., Choyke, P., Turkbey, B., Pinto, P., Wood, B.J., Kruecker, J.: Realtime TRUS/MRI fusion targeted-biopsy for prostate cancer: A clinical demonstration of increased positive biopsy rates. In: Madabhushi, A., Dowling, J., Yan, P., Fenster, A., Abolmaesumi, P., Hata, N. (eds.) MICCAI 2010. LNCS, vol. 6367, pp. 52–62. Springer, Heidelberg (2010)
9. Karnik, V.V., Fenster, A., Bax, J., Cool, D.W., Gardi, L., Gyacskov, I., Romagnoli, C., Ward, A.D.: Assessment of image registration accuracy in three-dimensional transrectal ultrasound guided prostate biopsy. Med. Phys. 37(2), 802–813 (2010)

10. Kim, J.H., Kim, J.K., Park, B.W., Kim, N., Cho, K.S.: Apparent diffusion coefficient: prostate cancer versus noncancerous tissue according to anatomical region. J. Magn. Reson. Imaging 28(5), 1173–1179 (2008)
11. Kitajima, K., Kaji, Y., Fukabori, Y.: Prostate cancer detection with 3 T MRI: comparison of diffusion-weighted imaging and dynamic contrast-enhanced MRI in combination with T2-weighted imaging. J. Magn. Reson. Imaging 31(3), 625–631 (2010)
12. Kvåle, R.: Concordance between Gleason scores of needle biopsies and radical prostatectomy specimens: a population-based study. BJU Int. 103(12), 1647–1654 (2009)
13. Martin, S., Baumann, M., Daanen, V., Troccaz, J.: MR prior based automatic segmentation of the prostate in TRUS images for MR/TRUS data fusion. In: Proceedings of the 2010 IEEE international conference on Biomedical imaging: From Nano to Macro, ISBI 2010, pp. 640–643. IEEE Press, Piscataway (2010)
14. Miyagawa, T., Ishikawa, S., Kimura, T., Suetomi, T., Tsutsumi, M., Irie, T., Kondoh, M., Mitake, T.: Real-time virtual sonography for navigation during targeted prostate biopsy using magnetic resonance imaging data. Int. J. Urol. 17(10), 855–860 (2010)
15. Roehl, K.A., Antenor, J.A.V., Catalona, W.J.: Serial biopsy results in prostate cancer screening study. J. Urol. 167(6), 2435–2439 (2002)
16. Singh, A.K., Kruecker, J., Xu, S., Glossop, N., Guion, P., Ullman, K., Choyke, P.L., Wood, B.J.: Initial clinical experience with real-time transrectal ultrasonography-magnetic resonance imaging fusion-guided prostate biopsy. BJU Int. 101(7), 841–845 (2008)
17. Tamada, T., Sone, T., Jo, Y., Toshimitsu, S., Yamashita, T., Yamamoto, A., Tanimoto, D., Ito, K.: Apparent diffusion coefficient values in peripheral and transition zones of the prostate: comparison between normal and malignant prostatic tissues and correlation with histologic grade. J. Magn. Reson. Imaging 28(3), 720–726 (2008)
18. Tanimoto, A., Nakashima, J., Kohno, H., Shinmoto, H., Kuribayashi, S.: Prostate cancer screening: the clinical value of diffusion-weighted imaging and dynamic MR imaging in combination with T2-weighted imaging. J. Magn. Reson. Imaging 25(1), 146–152 (2007)